

# Strong Room Temperature 505 nm Emission from Hexagonal Crack Free InGaN Thin Film on Si(111) Grown by MBE

L. S. Chuah <sup>a,\*</sup>, Z. Hassan <sup>b</sup>, C. W. Chin <sup>b</sup>, M. Hussein Mourad <sup>b</sup>, F. K. Yam <sup>b</sup> and S. S. Ng <sup>b</sup>

<sup>a</sup> Physics Section, School of Distance Education, Universiti Sains Malaysia, 11800 Penang, Malaysia
<sup>b</sup> School of Physics, Universiti Sains Malaysia, 11800 Minden, Penang, Malaysia

Received 10 January 2010; accepted 24 June 2010

#### Abstract

GaN growth on Si(111) substrate typically routes to the initial high dislocation density and cracks because of the large discrepancy of lattice constant and thermal expansion coefficient between GaN and Si. This article reports the use of plasma-assisted molecular beam epitaxy (MBE) to grow crack-free InGaN on Si(111) substrate using an optimized GaN/AlN buffer layer. X-ray diffraction revealed that monocrystalline InGaN was obtained. To assess the morphology of the sample, scanning electron microscopy (SEM) and atomic force microscopy (AFM) have been employed. A layer-cracking problem was not observed in our samples. The root–mean–square (rms) roughness value of the surfaces sample is 10.34 nm on a 10  $\mu m \times 10~\mu m$  scan area. The film is then characterized by photoluminescence (PL) spectroscopy. PL measurement exhibits a sharp and intense band edge emission of InGaN with yellow luminescence (YL), red luminescence (RL) and near infrared luminescence (NIRL) peaks. To date, no approaches have been reported that YL is observed in samples grown by MBE.

© Koninklijke Brill NV, Leiden, 2011

#### Keywords

MBE, PL, InGaN, GaN, Si(111)

## 1. Introduction

GaN-based materials display a great deal of promise when used at various concentrations due to their potential applications for optoelectronic devices operating in the whole visible spectral range and in electronic devices, for example in high power, high temperature and high frequency transistors. The wide band-gap nitride semiconductors, such as InN, GaN, AlN have direct band-gaps of 0.7 eV (near IR), 3.4 eV (mid UV) and 6.2 eV (deep UV), respectively. Band-gaps that are variable from 0.7 eV to 6.2 eV can be realized through proper alloy combinations in the

<sup>\*</sup> To whom correspondence should be addressed. E-mail: chuahleesiang@yahoo.com

alloy system (InGaN, InAlN and AlGaN) starting from which quantum wells may be formed.

InGaN has been particularly intensively investigated amongst the ternary compounds of Group III-nitride materials. InGaN-based compounds have been recognized as being one of the utmost significant and important materials applied for the fabrication of light emitters. InN is viewed to be an extremely promising material for the forthcoming photonic and electronic devices as a result of its prominent material properties, like smallest effective mass, highest peak, largest mobility and, smallest direct band-gap. In spite of the recent notable advance in InGaN technology, nevertheless, the basic physics related to the InGaN materials has not been well developed. Some of the physical and chemical properties are still adjudged based on GaN and InN, for example, lattice parameters, elastic constants, the band structure, electron density of states and other properties [1].

In addition, the band-gap energy of InN has been experimentally measured indicates that the fundamental band-gap is around 0.7 eV [2–7]. However, there is still debate on the correct fundamental band gap. Several groups [8–10] have suggested that the InN band gap is between 1.1 and 1.5 eV and have presented experimental data to substantiate their claim. Recently, the basic characteristics of GaN have been well documented, and there are many significant abstract papers about GaN and related materials, as can be discovered from the literature (see Refs [11–18]. Following a discussion of the structural properties of these materials, their electrical and optical properties have been described in detail. By contrast, the study of InN is still at a very early stage. This make the study of InGaN much more complex [1, 19–21].

The use of MBE for the growth of GaN-based materials, in fact, has a number of advantages as compared to metal organic chemical vapour deposition (MOCVD). For instance, low temperature growth, precise control of thickness and composition, *in situ* characterization capability, ultra-high vacuum (UHV) environment, and the use of high-purity materials, which minimize the presence of contaminants in the grown layers, in particular carbon, oxygen and hydrogen. However, the growth rate of MBE, was  $0.1\text{--}0.20~\mu\text{m/h}$ , is the principal weak point compared with other growth methods [22, 23].

It is well recognized that the structural, optical, and electrical characteristics of InGaN alloys could be vitally influenced by the growth conditions. An understanding of the end-use applications of InGaN is of enormous significance, because a small modification of the development parameters can produce a large difference in the quality of the InGaN thin film [1].

Because of the large differences in lattice constant and thermal expansion coefficient, the quality of GaN epitaxial layers on Si has been poorer if compared with that of sapphire and silicon carbide, and the trend of silicon to form an amorphous silicon nitride layer when exposed to reactive nitrogen sources. Since Si has a diamond structure, there are three commonly used faces of Si substrates with directions of (001), (011) and (111). In the choice between (001) and (111) faces for Si sub-

strates, it is the latter that are usually used for GaN epitaxy. In addition, Si itself displays resistivity up to  $10^4~\Omega$  cm, which is significantly less than the resistivity value of sapphire, SiC or GaN, and this could lead to parasitic capacitance effects in the middle of a high frequency operation. In nearly all cases, the Si(111) face is selected due to its trigonal order favouring epitaxial growth of the GaN(0001) face.

This article reports the use of plasma-assisted molecular beam epitaxy (MBE) to grow crack-free InGaN on Si(111) substrate using an optimized GaN/AlN buffer layer. To assess the optical and morphology of samples, X-ray diffraction (XRD), scanning electron microscopy (SEM), atomic force microscopy (AFM) and photoluminescence (PL) spectroscopy have been employed.

## 2. Experimental

The growth of the InGaN/GaN/AlN film on Si(111) substrate was performed in a Veeco Gen II MBE system. High purity material sources, for example aluminum (6N5), gallium (7N) and indium (7N), were used in the Knudsen cells. Nitrogen (7N purity) was channeled to RF source to create reactive nitrogen species. The plasma was operated at typical nitrogen pressure of  $1.5 \times 10^{-5}$  Torr under a discharge power of 300 W at 13.56 MHz radio frequency (RF).

The growth of Group III-nitrides on 3-inch Si(111) substrate starts with the standard cleaning procedure by using a standard Radio Corporation of America (RCA) cleaning method prior to loading into MBE load lock chamber. In the preparation chamber, the substrates were outgassed for 10 min at 400°C prior to growth.

After evacuation of the preparation chamber, the substrate was transferred into a growth chamber which was maintained at high vacuum and had provision for both growth and analysis. The growth chamber was equipped with a cryopump and the base pressure of the growth chamber was in the range of  $10^{-11}$  Torr. The cryopump, drifted by a helium compressor with a water-cooling system, was commonly maintained at 10 Kelvin and the pressure of the growth chamber was maintained in the range of  $10^{-11}$  Torr.

In the growth chamber, Si substrate was heated at 840°C, and then a few monolayers of Ga were deposited on the substrate for the purpose of removing the  $SiO_2$  by formation of  $GaO_2$ . A RHEED reconstruction with prominent Kikuchi lines is then observed, that turns into clean Si(111) surfaces at 840°C. Then a few atom monolayer of Al is deposited on silicon prior to the AlN buffer layer growth. A way to avoid the amorphous  $Si_xN_y$  layer formation is to start the growth with an AlN buffer layer, because the bond formation between Al and N atoms prevails over the Si–N one. It is well known that this buffer layer plays a critical function in determining the crystalline quality of the thin film. To grow the AlN buffer layer, the substrate temperature was heated up to 845°C, and both of the Al and N shutters were opened simultaneously for 15 min.

Subsequently, a GaN epilayer was grown on top of the AlN buffer layer for 20 min with substrate temperature set at 845°C. Immediately after the growth of

the GaN epilayer, the substrate temperature was ramped down to 700°C to make it ready for the growth of the InGaN epilayer. To grow InGaN, the effusion cells of In, and Ga were heated up to 1000°C and 1030°C, respectively. The growth duration for this InGaN epilayer was about 45 min.

To determine the exact orientation relationship and the content of the sample, high-resolution PANalytical X'Pert Pro MRD XRD system with a Cu  $K_{\alpha_1}$  radiation source ( $\lambda=1.5406$  Å) was used. The XRD pattern was scanned using the slow scan technique in the  $2\theta$  range of 20–80°, with a scan interval of 0.01° and step time of 1 s. The surface morphology of the samples was investigated by scanning electron microscopy (SEM) and atomic force microscopy (AFM). The optical quality of the film was investigated by photoluminescence (PL) at room temperature by using the Jobin Yvon HR800UV system, which is an integrated confocal micro photoluminescence spectrometer with He-Cd laser 325 nm as excitation source.

#### 3. Results and Discussion

The rigorous control of the conditions necessary for growing InGaN materials is a distinguishing feature as potentially there are many problems that could arise, such as the large inter-atomic spacing between GaN and InN which yields ascent to a solid phase miscibility gap [24, 25] and the comparatively high vapor pressure of InN [26]. Furthermore, the dissimilarity of enthalpies of formation for InN and GaN effect a hardy indium cover segregation on the growth front [20]. These barriers, still could be decreased by optimizing the growth parameters, for example, the usage of high V/III flux ratio, low growth rate and low growth pressure [1].

Figure 1 shows how the RHEED pattern changes during buffer layer (AlN) growth. Figure 1(a) shows a typical RHEED image at a few monolayers of Al. Figure 1(b)–(d) shows the RHEED images with 90 s, 5 and 15 min of AlN buffer layer growth. After 15 min of AlN buffer growth, a stable pattern which is different from Si(111) was formed. In this work, the sample was grown under Ga-stable conditions (Ga/N flux ratio greater than 1) that results in GaN growth. Growth of GaN by MBE utilizing high temperature buffer layer on Si(111) substrate nearly always produces a Ga-polar material. It is difficult to do experiments on both polarities of GaN using MBE, as in this study, when it is only conceivable to nucleate one polarity. Figure 2 shows a RHEED image of the InGaN layers. The films were found to be of good crystallinity as indicated by the streaky RHEED pattern, which indicates an atomically smooth surface.

Figure 3 shows the  $2\theta$  XRD spectra of the sample grown by MBE. The XRD measurement confirmed that the Group III-nitrides were epitaxially grown on Si(111). The intensity data were collected in two dimensions by performing an  $\omega$ - $2\theta$  scan at a range of different values. These can be seen from the presence of the peaks at  $34.48^{\circ}$ ,  $35.99^{\circ}$ ,  $72.84^{\circ}$  and  $76.47^{\circ}$ , which represent to GaN(0002), AlN(0002), GaN(0004) and AlN(0004), respectively. Besides that, a weak peak appears at  $32.83^{\circ}$  that can be attributed to InGaN(0002). The positions of the peaks

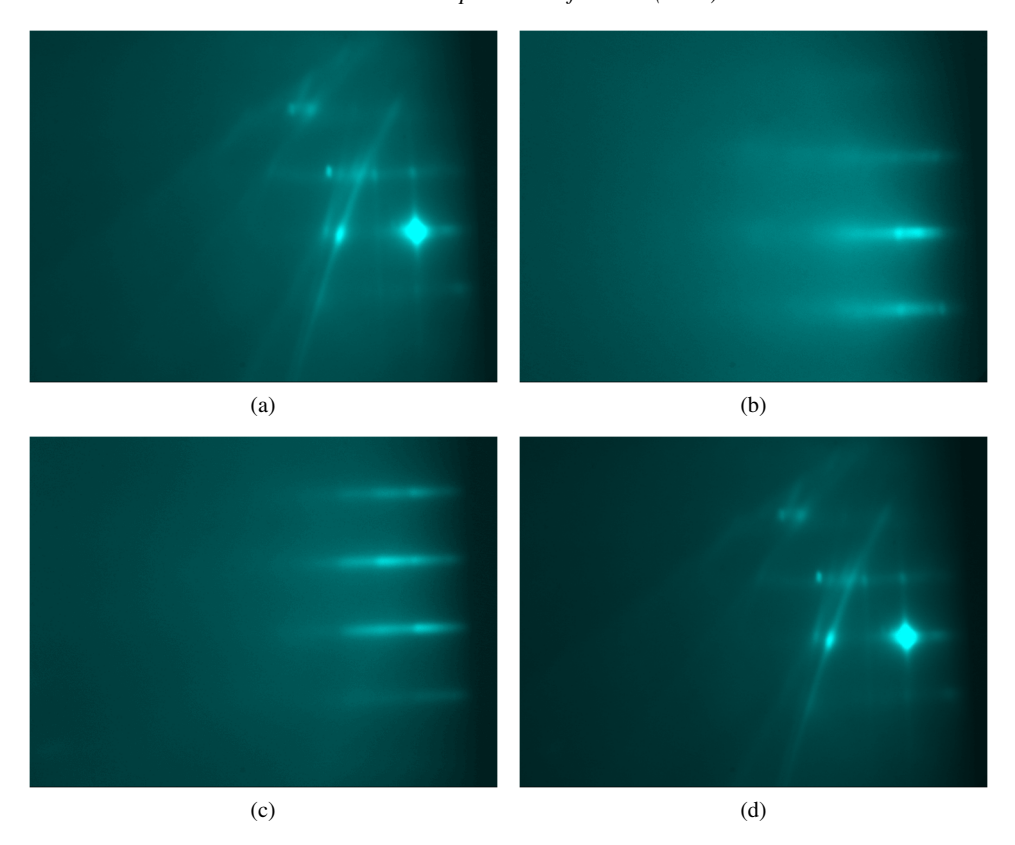


**Figure 1.** (a) Typical RHEED image at few monolayers of Al before AlN buffer layer growth. (b)–(d) Show the RHEED images with 90 s, 5 and 15 min of AlN layers.



Figure 2. RHEED image of the InGaN layers.

and the similar crystal planes as well as the relative intensity are put together in Table 1. The modeling of the  $\omega/2\theta$  XRD spectra showed that the thicknesses of the AlN, GaN and InGaN were 200, 250 and 50 nm, respectively; in addition, the

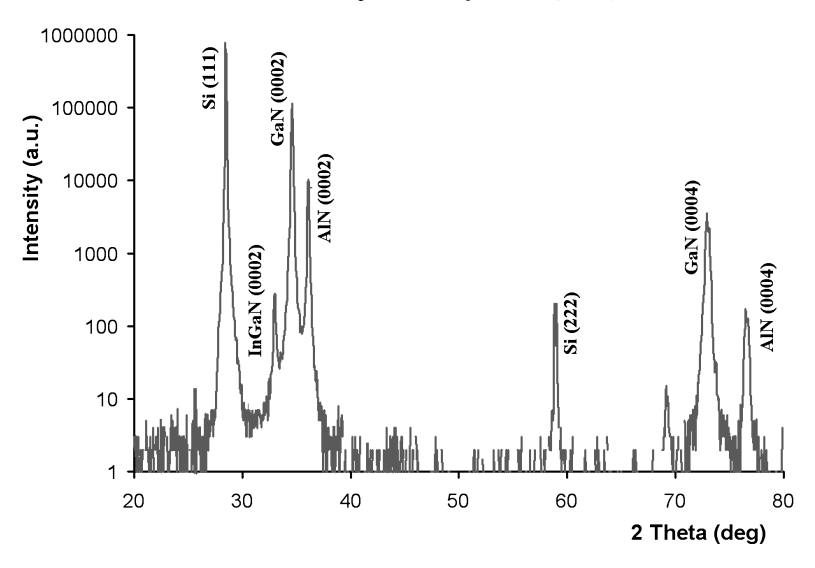


**Figure 3.** XRD spectra of the InGaN/GaN/AlN/Si sample by performing  $\omega$  (sample angle) —  $2\theta$  (detector angle) scan.

**Table 1.** The  $2\theta$  XRD peak positions of different crystal planes and their relative intensity

$2\theta$ peak position (°)	Crystal plane	Relative intensity (%)
28.36	Si(111)	100.00
32.83	InGaN	0.05
34.48	GaN(0002)	33.74
35.99	AlN(0002)	3.53
58.81	Si(222)	0.04
72.84	GaN(0004)	1.22
76.47	AlN(0004)	0.06

simulated result also revealed that the indium molar fraction of InGaN epilayer was 0.26.

The morphology of the InGaN films was characterized by plane-view scanning electron micrographs (SEM). As seen in Fig. 4, the surface of the sample consists of uniform, oriented grains that coalesce well into each other. Because of the lower deposition temperature in comparison to MOCVD, layer-cracking issues were not obtained in our samples. The surface roughness of InGaN sample was measured by AFM (Fig. 5). The root–mean–square (rms) roughness value of the surfaces sample is 10.34 nm on a  $10 \, \mu m \times 10 \, \mu m$  scan area.

We found that this optimized GaN/AlN buffer layer conditions are the best growth conditions to get crack-free InGaN on Si(111) substrate. In order to optimize

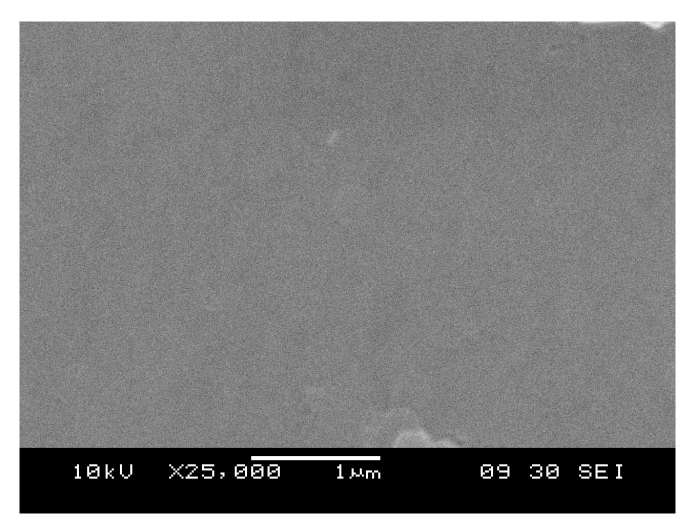


Figure 4. SEM image of the crack-free InGaN thin film.

the AlN buffer layer, the growth temperature and stoichiometry have to be carefully considered. Lower growth temperatures lead to an increasing surface roughness. If the buffer layer were too thin (<100 nm), the buffer action would not be very effective and the InGaN film becomes polycrystalline. On the other hand, if the buffer layer was somewhat thicker, the orientation correlation between the InGaN and the Si substrate could not be established.

PL spectroscopy is a good characterization tool to identify the appearance of defect related levels or defect induced luminescence in the sample. Figure 6 shows the room temperature PL spectrum (330-1000 nm) of InGaN on Si(111) substrate using an optimized GaN/AlN buffer layer. From Fig. 6, a strong near band edge emission for the sample is observed at 504.89 nm which is attributed to the band edge emission of InGaN. The PL spectra are dominated by an intense and sharp peak at 362.65 nm [27] which is attributed to the band edge emission of GaN and three defect-related luminescence peaks namely, yellow luminescence (YL), red luminescence (RL) and near infrared luminescence (NIRL) peaks. These defects induced luminescence peaks that are respectively observed at 556.19, 727.19 and 993.79 nm. To date, no investigations have reported that YL is observed in samples grown by MBE. This most probably is contaminated by residual Si (from the Si substrate). In addition, nitrogen vacancies (N<sub>Ga site</sub>) and gallium vacancies (Ga<sub>N site</sub>) are also two common defects in the GaN films [24, 25]. This led to the suggestion that the InGaN films contained these defect-related levels in the band-gap that may be the source of radiative recombination centres and leading to below band gap optical emission.

Vegard's law is commonly used to estimate the composition of ternary materials. The energy gap of  $In_xGa_{1-x}N$  is given by the composition-weighted average of the GaN and InN gaps, and can be approximated by

$$E_{g}(x) = xE_{g}(InN) + (1-x)E_{g}(GaN),$$
 (1)

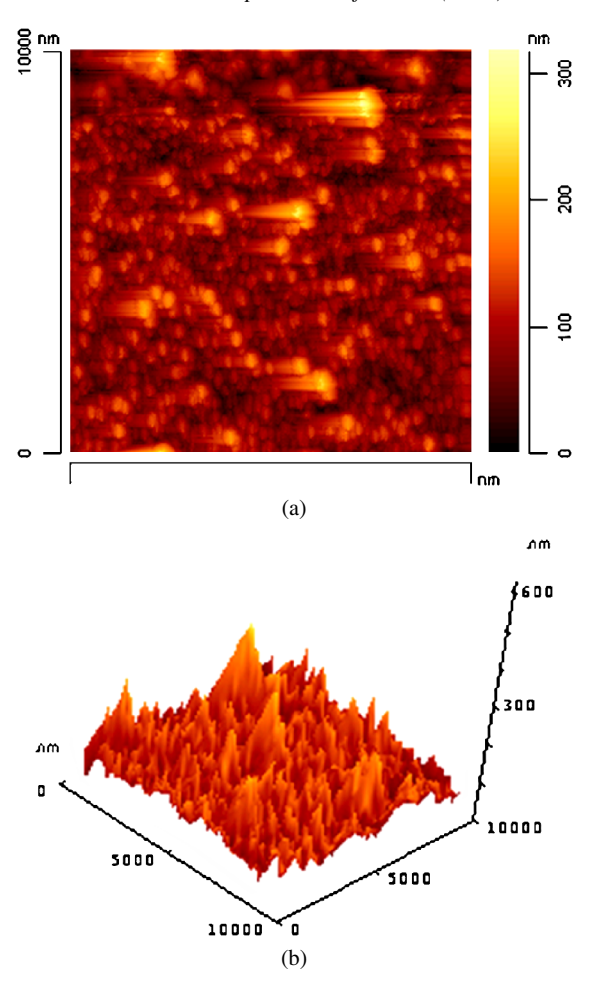


Figure 5. AFM micrograph of the InGaN thin film: (a) 2D and (b) 3D.

where the band-gap of wurtzite GaN and InN at 300 K are  $E_g(GaN) = 3.42$  eV,  $E_g(InN) = 0.77$  eV, respectively. Accuracy can be improved using this standard equation, in which a third term with a 'bowing' parameter, b, is added in:

$$E_{g}(x) = x E_{g}(InN) + (1 - x)E_{g}(GaN) - bx(1 - x)$$
 (2)

and the bowing parameter, b = 1.43 eV [1, 28]. Therefore, equation (2) becomes

$$2.46 = -4.08x + 3.42 + 1.43x^{2}$$

from which we obtain x = 0.26. This means that the percentage of In is about 26% and better described as  $In_{0.26}Ga_{0.74}N$ . This is in good agreement with the results of the XRD simulated result.

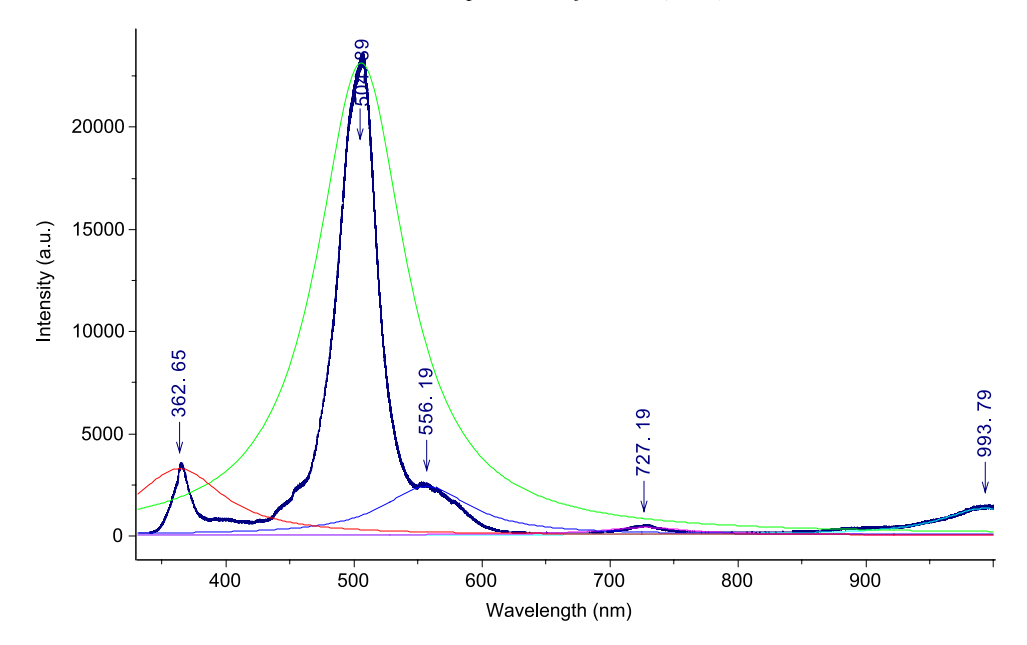


Figure 6. Room temperature micro-PL spectrum of InGaN sample together with Lorentzian model fits.

## 4. Conclusions

The growth of InGaN/GaN/AlN on Si(111) substrate has been performed using plasma-assisted molecular beam epitaxy. The optical property of the thin film has been analyzed by PL. The structural quality of the thin film is comparable to the values reported in the literature. Sharp and intense band edge emission of InGaN is observed in the PL measurement with yellow band emission.

## Acknowledgement

Support from Universiti Sains Malaysia is gratefully acknowledged.

#### References

- 1. F. K. Yam and Z. Hassan, InGaN: an overview of the growth kinetics, physical properties and emission mechanisms, *Superlattices and Microstructures* **43**, 1–23 (2007).
- 2. Y. Saito, H. Harima, E. Kurimoto, T. Yamaguchi, N. Teraguchi, A. Suzuki, T. Araki and Y. Nanishi, Growth temperature dependence of indium nitride crystalline quality grown by RF-MBE, *Phys. Stat. Sol. B* **234**, 796–800 (2002).
- 3. V. Yu. Davydov, A. A. Klochikhin, R. P. Seisyan, V. V. Emtsev, S. V. Ivanov, F. Bechstedt, J. Furthmuller, H. Harima, A. V. Mudryi, J. Aderhold, O. Semchinova and J. Graul, Absorption and emission of hexagonal InN Evidence of narrow fundamental band gap, *Phys. Stat. Sol. B* 229, R1–R3 (2002).
- 4. I. Vurgaftman, J. R. Meyer and L. R. Ram-Mohan, Band parameters for III–V compound semi-conductors and their alloys, *J. Appl. Phys.* **89**, 1368156–1368217 (2001).

- 5. B. Monemar, P. P. Paskov and A. Kasic, Optical properties of InN the band-gap question, *Superlattices and Microstructures* **38**, 38–56 (2005).
- B. Arnaudov, T. Pashkova, P. P. Paskov, B. Magnusson, E. Valcheva, B. Monemar, H. Lu, W. J. Schaff, H. Amano and I. Akasaki, Energy position of near-band-edge emission spectra of InN epitaxial layers with different doping levels, *Phys. Rev. B* 69, 115216–115220 (2004).
- W. Walukiewicz, S. X. Li, J. Wu, K. M. Yu, J. W. Ager III, E. E. Haller, H. Lu and W. J. Schaff, Optical properties and electronics structure of InN and In-rich group III-nitride alloys, *J. Cryst. Growth* 269, 119–127 (2004).
- 8. Q. X. Guo, T. Tanaka, M. Nishio, H. Ogawa, X. D. Pu and W. Z. Shen, Observation of visible luminescence from indium nitride at room temperature, *Appl. Phys. Lett.* **86**, 231913–231916 (2005).
- P. Specht, J. C. Ho, X. Xu, R. Armitage, E. R. Weber, R. Erni and C. Kisielowski, Band transitions in wurtzite GaN and InN determined by valence electron energy loss spectroscopy, *Solid State Comm.* 135, 340–344 (2005).
- K. S. A. Butcher, M. Winttrebert-Fouquet, P. P.-T. Chen, T. L. Tansley, H. Dou, S. K. Shrestha, H. Timmers, M. Kuball, K. E. Prince and K. E. Bradby, Nitrogen-rich indium nitride, <u>J. Appl.</u> Phys. 95, 6124–6128 (2004).
- 11. S. J. Pearton, J. C. Zolper, R. J. Shul and F. Ren, GaN: processing, defects, and devices, <u>J. Appl. Phys.</u> **86**, 1–78 (1999).
- 12. S. J. Pearton, F. Ren, A. P. Zhang and K. P. Lee, Fabrication and performance of GaN electronics devices, *Mater. Sci. Engng R* **30**, 55–212 (2000).
- 13. S. N. Mohammad and H. Morkoc, Progress and prospects of group-III nitride semiconductors, *Prog. Quant. Electr.* **20**, 361–525 (1996).
- 14. Y. Sato, A. Kurosaki and S. Sato, Low-temperature growth of GaN and InGaN films on glass substrates, *J. Cryst. Growth* **189/190**, 42–46 (1998).
- 15. R. F. Davis, A. M. Roskowski, E. A. Preble, J. S. Speck, B. Heying, J. A. Feitas, E. R. Glaser Jr. and W. E. Carlos, Gallium nitride materials progress, status, and potential roadblocks, *Proc. IEEE* **90**, 993–1005 (2002).
- M. A. Reshchikov and H. Morkoc, Luminescence properties of defects in GaN, J. Appl. Phys. 97, 1–95 (2005).
- 17. O. Ambacher, Growth and applications of group III-nitrides, <u>J. Phys. D: Appl. Phys. 31</u>, 2653–2710 (1998).
- H. Morkoc, S. Strite, B. G. Gao, M. E. Lin, B. Sverdlov and M. Burns, Large band gap SiC, III–V nitride, and II–VI ZnSe based semiconductor device technologies, *J. Appl. Phys.* 76, 1363–1398 (1994).
- A. G. Bhuiyan, A. Hashimoto and A. Yamamoto, Indium nitride (InN): a review on growth, characterization, and properties, *J. Appl. Phys.* 94, 2779–2808 (2003).
- T. Matsuoka, Progress in nitride semiconductors from GaN to InN–MOVPE growth and characteristics, Superlattices and Microstructures, 37, 19–32 (2005).
- Y. Nanishi, Y. Saito and T. Yamaguchi, RF-molecular beam epitaxy growth and properties of InN and related alloys, *Japan J. Appl. Phys.* 42, 2549–2559 (2003).
- H. Sakai, T. Koide, H. Suzuki, M. Yamaguchi, S. Yamasaki, M. Koike, H. Amano and I. Akasaki, GaN/GaInN/GaN double heterostructure light emitting diode fabricated using plasma-assisted molecular beam epitaxy, *Japan J. Appl. Phys.* 34, L1429–L1431 (1995).
- 23. P. Laukkanen, S. Lehkonen, P. Usimaa, M. Pessa, A. Sepala, T. Ahlgren and E. Rauhala, Emission studies of InGaN layers and LEDs grown by plasma-assisted MBE, *J. Cryst. Growth* **230**, 503–506 (2001).

- 24. O. Ambacher, Growth and applications of group III-nitrides, <u>J. Phys. D: Appl. Phys. 31</u>, 2653–2710 (1998).
- 25. H. Morkoc, S. Strite, B. G. Gao, M. E. Lin, B. Sverdlov and M. Burns, Large band-gap SiC, III–V nitride, and II–VI ZnSe-based semiconductor device technologies, *J. Appl. Phys.* **76**, 1363–1398 (1994).
- 26. A. G. Bhuiyan, K. Sugita, K. Kasashima, A. Hashimoto, A. Yamamoto and V. Yu. Davydov, Single-crystalline InN films with an absorption edge between 0.7 and 2 eV grown using different techniques and devices and evidence of the actual band-gap energy, *Appl. Phys. Lett.* 83, 4788–4790 (2003).
- G. Popovici and H. Morkoc, Growth and doping of defects in III-nitrides, in: *GaN and Related Materials II*, Ch. 3, S. J. Pearton (Ed.), pp. 93–172. Gordon and Breach Science Publisher, UK (2000).
- E. L. Piner, F. G. McIntosh, J. C. Roberts, M. E. Aumer, V. A. Joshkin, S. M. Bedair and N. A. El Masry, Model for indium incorporation in the growth of InGaN film, *Mat. Res. Soc. Symp. Proc.* 449, 85–88 (1997).